



## RESEARCH ARTICLE

### EXPLORING MESOMORPHIC PROPERTIES AND THERMAL BEHAVIOR OF NOVEL THERMOTROPIC LIQUID CRYSTALS FEATURING BROMO-SUBSTITUTED TERMINAL GROUPS AND AZO-EMBEDDED CHALCONYL ESTER LINKAGES THROUGH SYNTHESIS AND CHARACTERIZATION

\*Pushparajsinh P. Zala and Umed C. Bhoya

Department of Chemistry, Saurashtra University, Rajkot-360005, Gujarat, India

#### ARTICLE INFO

##### Article History:

Received 19<sup>th</sup> April, 2024  
Received in revised form  
15<sup>th</sup> May, 2024  
Accepted 20<sup>th</sup> June, 2024  
Published online 29<sup>th</sup> July, 2024

##### Key words:

Mesophases, Ethyl Spacer,  
Nematic, Smectic, Dsc.

##### \*Corresponding author:

Pushparajsinh P. Zala

#### ABSTRACT

In this research, a novel set of azoester derivatives featuring a bromo terminal group was synthesized and meticulously characterized to assess their mesomorphic characteristics. These compounds were synthesized via esterification reaction involving 4-n-alkoxy-3-methoxy cinnamic acid and 4-((4-bromophenyl) diazenyl)-2-methylphenol. Analysis revealed 12 distinct derivatives displaying predominantly nematogenic behavior, with mesophase initiation observed from the earliest homologue. The mesophase span varied from 4.8°C to 30.9 °C. The decline in the isotropic temperature of the liquid crystal (LC) compounds with increasing carbon chain length underscored the impact of chain flexibility. Various characterization techniques including Fourier-transform infrared spectroscopy (FT-IR), mass spectroscopy, proton nuclear magnetic resonance (<sup>1</sup>H-NMR), Gauss view, and elemental analysis were employed to probe the compounds' attributes. Polarized optical microscopy (POM) confirmed the presence of mesogenic phases, while differential scanning calorimetry (DSC) elucidated the thermal properties of select homologues. Additionally, a comparative analysis of the mesomorphic behaviors of the novel azoester series with structurally akin series was conducted, yielding insights into their distinctive properties and potential applications. This study contributes significantly to the comprehension of the intricate relationship between molecular structure and mesophase behavior, providing crucial groundwork for the future design and advancement of liquid crystal materials.

Copyright©2024, Pushparajsinh P. Zala and Umed C. Bhoya. This is an open access article distributed under the Creative Commons Attribution License, which permits unrestricted use, distribution, and reproduction in any medium, provided the original work is properly cited.

Citation: Pushparajsinh P. Zala and Umed C. Bhoya. 2024. "Exploring mesomorphic properties and thermal behavior of novel thermotropic liquid crystals featuring bromo-substituted terminal groups and azo-embedded chalconyl ester linkages through synthesis and characterization". *International Journal of Current Research*, 16, (07), 29137-29143.

## INTRODUCTION

Liquid crystals (LCs) represent a unique state of matter, exhibiting properties that bridge those of conventional liquids and solids, characterized by ordered arrangements that confer distinctive optical traits like birefringence and dichroism.[1] The study of LCs is expanding rapidly, with applications ranging from biomedical carriers to display devices and semiconductor materials. Since its establishment in 1888[2]-[6], the field of LCs has been the focus of significant scientific inquiry. In this investigation, we explore the mesomorphic characteristics of a series of homologues sharing the molecular structure RO-C<sub>6</sub>H<sub>3</sub>(-OCH<sub>3</sub>)-CH=CH-COO-C<sub>6</sub>H<sub>3</sub>(-CH<sub>3</sub>)-N=N-C<sub>6</sub>H<sub>3</sub>-Br. Our research identifies a novel liquid crystal compound distinguished by reduced crystallinity, heightened solubility, and an intermediate melting point. This compound shares similarities with other LCs featuring terminal polar groups such as Chlorine (Cl), Fluorine (F), Bromine (Br), and Iodine (I). [2] The introduction of a bromo group enhances molecular polarizability, influencing intramolecular interactions and potentially inducing polymorphic behavior.

The reduction in crystallinity observed in the compound can be attributed to the presence of the bromo group, which disrupts the regular molecular arrangement within the crystal lattice. Consequently, a less ordered structure emerges, leading to a lower melting point and enhanced solubility of the compound. The remarkable solubility is likely facilitated by the polar nature of the bromo group, enabling interactions with solvent molecules and promoting dissolution.[2] The synthesized series comprises 12 homologues, each distinguished by an additional methylene group. An ethyl spacer connects the -COO- and -N=N- moieties, with a bromo group terminating one end and an n-alkyl chain at the other. Introduction of the ethyl spacer extends the molecular length, imparting a more linear and flexible configuration. Through comprehensive analytical characterization and assessment using polarizing optical microscopy, the synthesized homologues' physical properties were thoroughly examined.[7]-[9]

## MATERIALS AND METHODS

The synthesis involved various chemicals and solvents sourced from Spectrochem, Merck, and Sigma-Aldrich, including

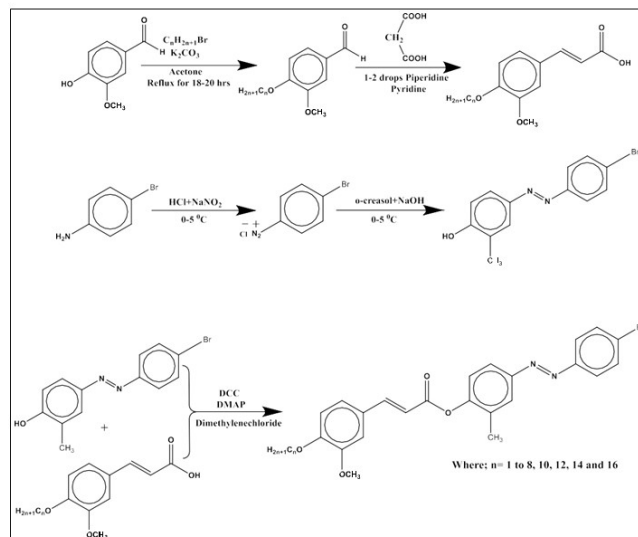
4-Hydroxy-3-methoxy benzaldehyde, n-alkyl bromides (R-Br), K<sub>2</sub>CO<sub>3</sub>, malonic acid, dicyclohexylcarbodiimide (DCC), 4-Dimethylaminopyridine (DMAP), 2-bromo benzaldehyde, 4-hydroxy acetophenone, NaOH, pyridine, and piperidine. These reagents and solvents were utilized without purification. The purity of the synthesized compounds was confirmed via Thin-Layer Chromatography (TLC) employing 0.2 mm pre-coated silica gel G60 F254 plates (Merck), with visualization under UV light at wavelengths of 256 nm and 366 nm. A representative subset of the novel series underwent elemental analysis using the EuroEA Elemental Analyzer. Infrared (IR) spectra were recorded using a Shimadzu FTIR-8400 spectrometer. Proton nuclear magnetic resonance (<sup>1</sup>H NMR) and carbon-13 nuclear magnetic resonance (<sup>13</sup>C NMR) spectra were obtained utilizing a Bruker spectrometer with DMSO-d<sub>6</sub> as the solvent. Mass spectra were recorded using a Shimadzu GC-MS Model No. QP-2010.

**Preparation of 4-n-Alkoxy Cinnamic Acid [Int-A]:** The synthesis of 4-n-Alkoxy cinnamic acid (A-I) involved the Verley-Doebner modification of the Knoevenagel condensation method. In a 25-mL round-bottom flask, 4-n-alkoxy benzaldehyde (0.1 mol) and malonic acid (0.2 mol) were dissolved in pyridine (25 mL) with a few drops of piperidine. The mixture was refluxed for 2 hours under appropriate ventilation in a fume hood. [10] Following reflux, the solution was carefully poured into a 2M HCl aqueous solution and allowed to cool to room temperature. The resulting solid precipitate was collected via filtration, washed with water, and subjected to recrystallization from methanol until a pure single spot product was obtained. The resulting 4-n-Alkoxy cinnamic acids were confirmed to be trans isomers.[11]

**Synthesis of 4-((4-bromophenyl) diazenyl)-2-methyl phenol [Int-B]:** The synthesis of 4-((4-bromophenyl) diazenyl)-2-methyl phenol (Int-B) began with the measurement and weighing of 4-Bromoaniline (1 equivalent) in a 500 mL beaker. The compound was then combined with a mixture of hydrochloric acid (HCl) and water, and magnetic stirring was utilized in an ice bath until complete dissolution of the solid occurred. Meanwhile, in a separate container, an appropriate quantity of sodium nitrite (NaNO<sub>2</sub>) was dissolved in water and cautiously added to the reaction mixture. The resulting mixture was stirred for 1 hour. Concurrently, phenol (1 equivalent) and sodium hydroxide (NaOH) were dissolved in water, and after cooling, the two solutions were gradually blended together. Stirring continued for over an hour until the reaction was complete, resulting in the formation of a yellow-colored precipitate. To isolate the desired product, the mixture underwent vacuum filtration, yielding a crude product that was further purified via recrystallization in ethanol. The overall yield of the reaction was determined to be 72.6%.

**Synthesis of 4-(4'-n-Alkoxy-3'-methoxy cinnamoyloxy) 2-methyl azo 4''-bromo benzene:** In a 250 mL single-neck round-bottom flask (RBF), a solution of 4-n-Alkoxy-3-methoxycinnamic acid (Int-A) in an appropriate dichloromethylene solvent was prepared. Dicyclohexylcarbodiimide (DCC) (1.2 equivalents) and a small amount of 4-dimethylaminopyridine (DMAP) were introduced into the reaction mixture, followed by stirring at room temperature for 1 hour. Subsequently, 4-((4-Bromophenyl)diazenyl)-2-methyl phenol (Int-B) (1 equivalent) was added, and the solution was stirred for 24 hours at room

temperature [12]. The progression of the reaction was monitored using thin-layer chromatography (TLC). Upon completion of the reaction, vacuum filtration was employed to remove any precipitated dicyclohexylurea (DCU), followed by solvent evaporation using a rotary evaporator. The resulting crude product underwent recrystallization in ethanol. The percentage yield of each homologue was determined and is summarized in Table 1.



**Scheme 1. Synthesis Route of novel azoester series B-n**

The series members underwent comprehensive characterization employing various analytical methods. Elemental analysis was utilized to ascertain the elemental composition of the samples. Infrared (IR) spectra were recorded to delineate the functional groups within the samples. Proton nuclear magnetic resonance (<sup>1</sup>H NMR) spectra were acquired to provide intricate details about the molecular structures. Mass spectra were conducted to identify the molecular weights and fragmentation patterns. Thermal behavior was investigated via Differential Scanning Calorimeter (DSC) to determine key thermal properties such as melting and boiling points, as well as the glass transition temperature. Mesomorphic properties were examined using polarized optical microscopy to observe different phases and optical properties. The results from these analytical techniques were employed to thoroughly characterize the series members, offering insights into their chemical and physical attributes. Such information holds significant value for future studies and the exploration of novel applications for these compounds.

## CHARACTERIZATION

Characterization of the series involved employing diverse analytical methods. Elemental analysis was utilized to ascertain the composition of the samples. Infrared (IR) spectroscopy was employed to detect the functional groups present. Proton nuclear magnetic resonance (<sup>1</sup>H NMR) spectroscopy provided detailed insights into the molecular structure. Mass spectrometry aided in identifying molecular weight and fragmentation patterns. Differential Scanning Calorimetry (DSC) was used to explore thermal behavior, including melting and boiling points, as well as glass transition temperature. Polarized optical microscopy was employed to observe mesomorphic properties, visualize phases, and assess optical characteristics. Integration of these techniques facilitated comprehensive characterization, offering valuable insights into the chemical and physical properties of the series.

Such information is pivotal for future investigations and the development of novel applications for these compounds.

#### Analytical data: Elemental analysis

#### Spectral data

**<sup>1</sup>H NMR (CDCl<sub>3</sub>) of Pentoxyl derivative (B-5):** 0.89-0.96 (t, 3H, -CH<sub>3</sub> of -OC<sub>5</sub>H<sub>11</sub> group), 3.82-3.86 (s, 3H, -CH<sub>3</sub> of -O-CH<sub>3</sub> group), 1.35-1.75 (m, 6H, CH<sub>3</sub>-CH<sub>2</sub>-CH<sub>2</sub>-CH<sub>2</sub>-CH<sub>2</sub>-O-), 3.85-4.12 (t, 2H, -O-CH<sub>2</sub>), 6.24-6.42 (d, 1H, -COO-CH=CH-), 7.46-7.52 (d, 1H, -COO-CH=CH-), 2.30-2.35 (s, 3H, -CH<sub>3</sub> of Ph-CH<sub>3</sub> group) 7.75-7.98 (d, 4H, phenyl ring with -Br group), 7.24-7.85 (3H, middle phenyl ring), 7.00-7.08 & 7.20-7.30 (3H, phenyl ring with alkoxy chain). The <sup>1</sup>H NMR information corresponds faithfully to the molecular arrangement.

**<sup>1</sup>H NMR (CDCl<sub>3</sub>) of Heptoxyl derivative (B-7):** 0.86-0.94 (t, 3H, -CH<sub>3</sub> of -OC<sub>7</sub>H<sub>15</sub> group), 3.82-3.87 (s, 3H, -CH<sub>3</sub> of -O-CH<sub>3</sub> group), 1.35-1.78 (m, 10H, CH<sub>3</sub>-CH<sub>2</sub>-CH<sub>2</sub>-CH<sub>2</sub>-CH<sub>2</sub>-CH<sub>2</sub>-CH<sub>2</sub>-O-), 3.90-4.14 (t, 2H, -O-CH<sub>2</sub>), 6.28-6.40 (d, 1H, -COO-CH=CH-), 7.45-7.50 (d, 1H, -COO-CH=CH-), 2.32-2.36 (s, 3H, -CH<sub>3</sub> of middle Ph-CH<sub>3</sub> group), 7.78-7.98 (m, 4H, phenyl ring with -Br group), 7.24-7.84 (m, 3H, middle phenyl ring), 7.00-7.08 & 7.20-7.30 (m, 3H, phenyl ring with alkoxy chain). The <sup>1</sup>H NMR information corresponds faithfully to the molecular arrangement.

**<sup>13</sup>C NMR (CDCl<sub>3</sub>) in ppm for Butyloxy derivative (B-4):** 14.1 (-CH<sub>3</sub>), 22.7-31.9 (CH<sub>3</sub>-CH<sub>2</sub>)<sub>4</sub>, 69.0 (-OCH<sub>2</sub>), 56.1 (Ph-OCH<sub>3</sub>) 147.9 (-CH=CH-COO-), 115.5 (-CH=CH-COO-), 164.3 (-CH=CH-COO-), 17.8 (middle Ph-CH<sub>3</sub>), 111-158 (Ar-C). The <sup>13</sup>C NMR data is reliable with the molecular structure.

**<sup>13</sup>C NMR (CDCl<sub>3</sub>) in ppm for Hexyloxy derivative (B-6):** 14.1 (-CH<sub>3</sub>), 22.5-32 (CH<sub>3</sub>-CH<sub>2</sub>)<sub>3</sub>, 68.7 (-OCH<sub>2</sub>), 56.1 (-OCH<sub>3</sub>) 147.8 (-CH=CH-COO-), 115.5 (-CH=CH-COO-), 164.3 (-CH=CH-COO-), 15.3 (middle Ph-CH<sub>3</sub>), 110-159 (Ar-C). The <sup>13</sup>C NMR data is reliable with the molecular structure.

**Mass spectra of Octyloxy derivative (B-8):** m/z: 579.9 (M)<sup>+</sup>, 288.9 (base peak), The mass spectra and data is reliable with the molecular structure.

**Mass spectra of Decanyloxy derivative (B-10):** m/z: 607.8 (M)<sup>+</sup>, 317.0 (100%, base peak), The mass spectra and data is reliable with the molecular structure.

**IR (KBr) in cm<sup>-1</sup> for Ethoxy derivative (B-6):** 3030-2978 (C-H str. of alkene disubstituted), 1728.28 (C=O str. of carbonyl carbon of ester group), 1589.40, 1620 (C=C str. of alkene), 1606, 1514 & 1473.66 (C=C str. of aromatic ring), 1325 & 1290 (C-H bending of alkene disubstituted), 1257.63 (C-O str. of ether linkage), 1124.47 (C-O str. of ester group), 1018.45, 972.16 & 833.28 (C-H bending of alkene), 540.09 (C-Br str.). The IR data is reliable with the molecular structure.

**IR (KBr) in cm<sup>-1</sup> for Butyloxy derivative (B-8):** 3020-3150 (C-H stretching of alkene disubstituted), 2924.18 & 2840 (C-H str. of (-CH<sub>2</sub>)<sub>n</sub> group of -OC<sub>4</sub>H<sub>9</sub>), 1728.28 (C=O str. of carbonyl carbon of ester group), 1627.97 (C=C str. of alkene), 1589.40, & 1465.95 (C=C str. of aromatic ring), 1303 & 1265.35 (C-H bending of alkene disubstituted), 1226.77 (C-O str. of ether linkage), 1118.75 (C-O str. of ester group), 1003.02 & 964.44 (C-H bending of alkene), 524.66 (C-Br str.). The IR data is reliable with the molecular structure.

#### Representative spectra of synthesized compound

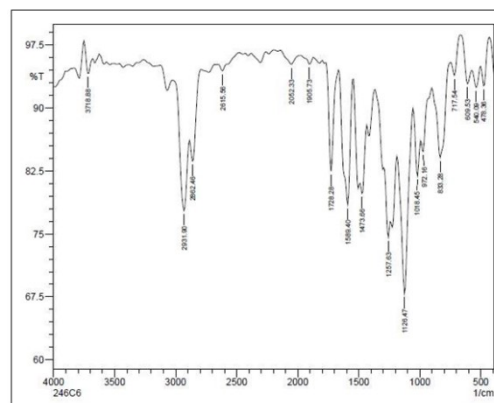


Figure 1. IR (KBr) in cm<sup>-1</sup> for Hexoxy derivative B6 IR

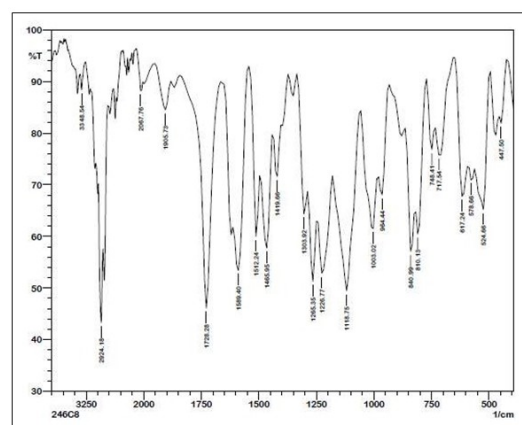


Figure 2. IR (KBr) in cm<sup>-1</sup> for octoxy derivative B8

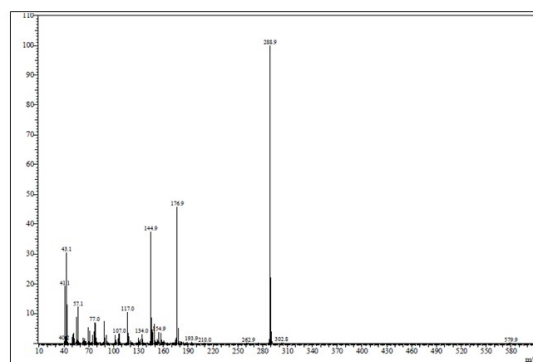


Figure 3 Mass spectra of Octyloxy derivative (B-8)

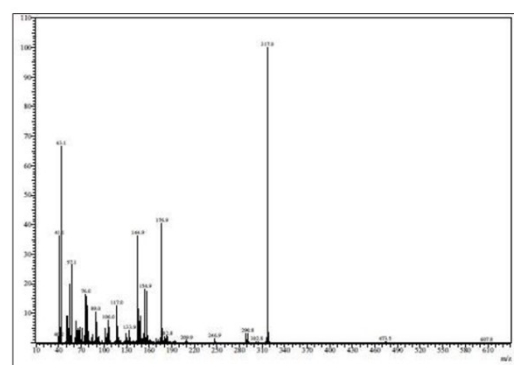


Figure 4 Mass spectra of Decanyloxy derivative (B-10)

## RESULTS AND DISCUSSION

In this study, a new set of chemical compounds sharing structural similarities, namely 4-(4'-n-Alkoxy-3'-methoxy cinnamoyloxy) 2-methyl phenyl azo 4''-bromo benzene, was synthesized via esterification involving two key intermediates: 4-n-Alkoxy-3-methoxy cinnamic acid [Int-A] and 4-((4-Bromophenyl)diazanyl)-2-methylphenol [Int-B]. While the intermediate compounds individually did not exhibit liquid crystalline properties, their combination led to the formation of a liquid crystalline phase. By systematically studying this series, a relationship between molecular structure and liquid crystal behavior was established. A total of twelve compounds were synthesized, and their respective phase transition temperatures were determined using a polarizing optical microscope (Nikon Eclipse 400/TU Plan ELWD 20X/0.40). The investigated compounds demonstrated nematogenic characteristics. The mesomorphic characteristics of the present series were explored using a polarizing optical microscope fitted with a heating plate. Sample preparation involved sandwiching approximately 1 mg of the compound between two glass plates via heat treatment, and the resulting assembly was subjected to analysis. The measurements for all homologues were meticulously recorded and tabulated in Table 2.

These data were then used to construct a transition graph, illustrating the correlation between transition temperature and the length of the n-alkyl chain. Analysis of the results presented in Table 2 revealed that the synthesized series displayed partial nematogenic properties. Specifically, the initial three homologues namely B-2, B-3 AND B-4 exclusively demonstrated a nematogenic phase below 180°C without exhibiting a smectogenic mesophase. The transition from a crystalline to an isotropic state was observed for all homologues at temperatures below 194 °C. These transition temperature values were utilized to generate the graphical representation depicted in Figure 5. Figure 5 presents the correlation between transition temperature, measured in degrees Celsius, and the number of carbon atoms within the flexible alkyl chain, delineating the liquid crystal (LC) phase behavior. The dotted line signifies the Cr-I transition curve. Compounds B-2 to B-4 exhibit the odd-even effect, which diminishes from B-8 to B-14. Regarding the Cr-N curve, the transition temperature consistently diminishes with an increase in the number of carbon atoms in the flexible n-alkyl chain, particularly evident from B-2 to B-4. Moreover, another odd-even effect manifests between the B-8 to B-14. homologues. Intriguingly, the odd-even effect and the decreasing trend alternate along the Cr-N transition.

**Table 1. Elemental Analysis of Homologous series B-n**

Sr.No.	Molecular Formula	Elements % Found			Elements % Calculated		
		C	H	O	C	H	O
1	C <sub>25</sub> H <sub>23</sub> BrN <sub>2</sub> O <sub>4</sub>	72.50	5.22	14.35	72.56	5.19	14.32
2	C <sub>31</sub> H <sub>35</sub> BrN <sub>2</sub> O <sub>4</sub>	74.06	6.24	2.73	74.02	6.21	12.72
3	C <sub>35</sub> H <sub>43</sub> BrN <sub>2</sub> O <sub>4</sub>	75.86	7.56	10.67	75.91	7.54	10.64

**Table 2. Phase transition temperature of series B-n in °C**

Compound	Flexible Chain	Sm(°C)	Nm(°C)	Isotropic(°C)
B-1	Methyl	-	-	192.3
B-2	Ethyl	-	(154.3)	185.2
B-3	Propyl	-	(159.2)	168.7
B-4	Butyl	-	(160.3)	165.1
B-5	Pentyl	-	-	157.8
B-6	Hexyl	-	-	143.2
B-7	Heptyl	-	-	139.2
B-8	Octyl	-	(123.0)	138.2
B-10	Decyl	-	(108.8)	116.8
B-12	Dodecyl	-	(106.8)	123.3
B-14	Tetradecyl	-	(102.5)	117.7
B-16	Hexadecyl	-	-	109.9

**Table 3. Molecular orbital energies, hardness ( $\eta$ ) and global softness (S) of B-1**

Compound	E <sub>HOMO</sub> (a.u)	E <sub>LUMO</sub> (a.u)	$\Delta E(E_{LUMO}-E_{HOMO})$ (a.u)	S = 1/ $\Delta E = (1/2\eta)$
Z-2	-0.05424	0.12896	0.07472	13.38

**Table 4. Commencement & Average transition temperature of series B-n and series- PCOCCA-n**

Series	B-n	PCOCCA-n
Smectic-Nematic	Not Applicable	124.2 °C (C2 & C14-C16)
Commencement of smectic phase	Not Applicable	C2
Nematic-Isotropic	130.7 °C (B2-B14)	139.4 °C (C1-C16)
Commencement of nematic phase	B2	C1
Total mesophase length in °C	30.9 °C B2	3.8 °C to 64.3 °C C1C2

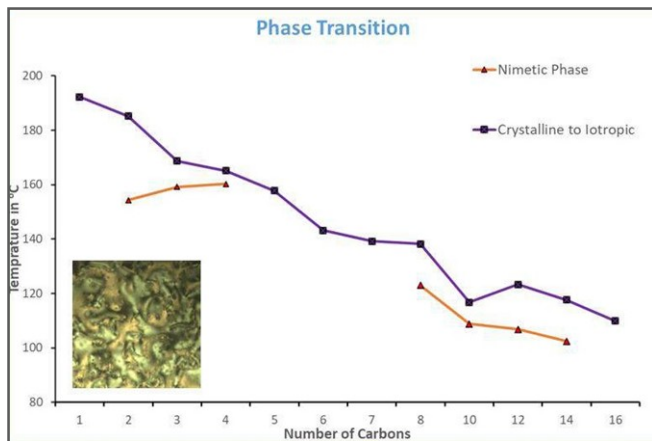


Figure 5. Phase Transition

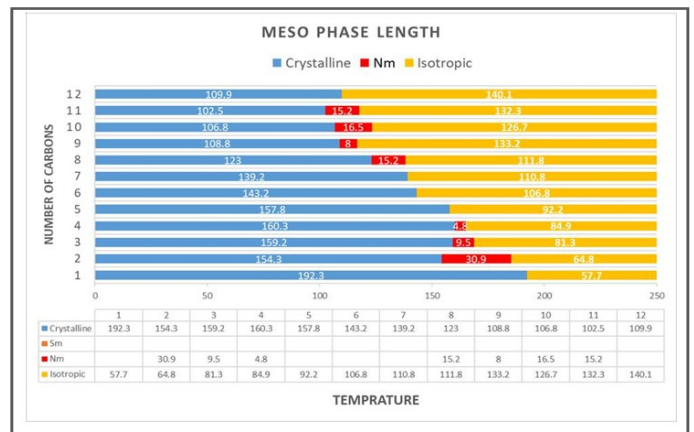
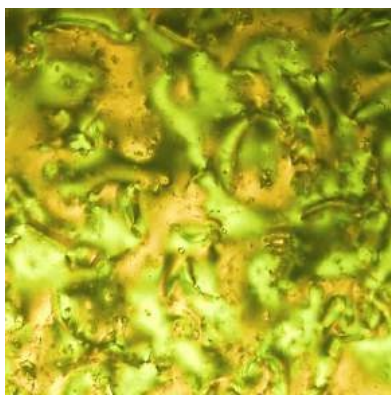
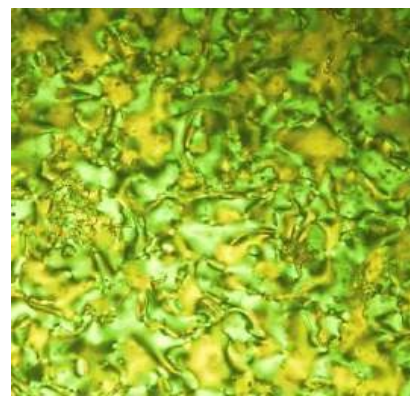


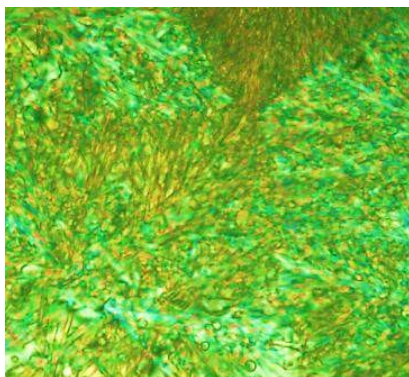
Figure 6. Mesophase Lengths diagram of series B-n



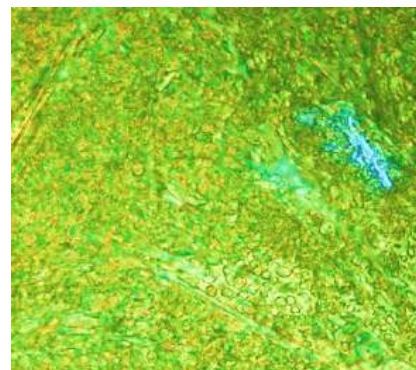
Nematic phase of B-2 Compound on heating scan



Nematic phase of B-8 Compound on heating scan



Nematic phase of B-10 Compound on heating scan



Nematic phase of B-14 Compound on heating scan

Figure 7. POM texture Analysis

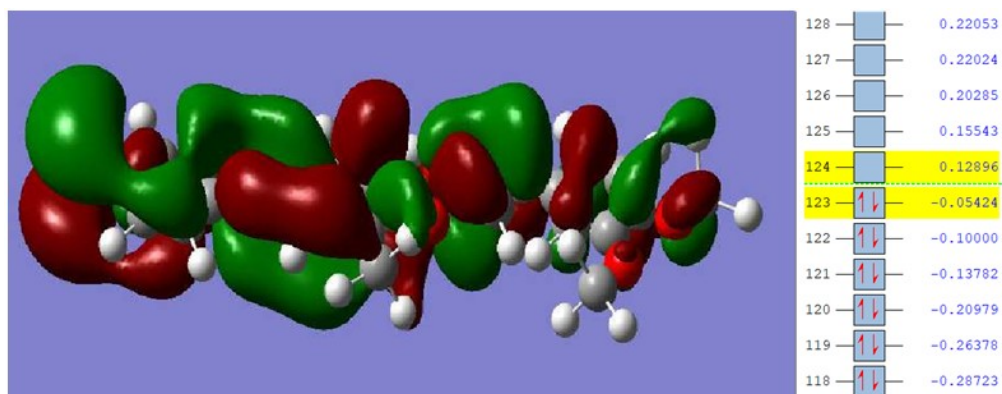


Figure 8. The calculated ground state isodensity surface plots for frontier molecular orbitals of B-1

Similarly, the N-I transition curve, also illustrated by a solid line, showcases a decreasing trend with an increasing number of carbon atoms in the n-alkyl chain. The N-I transition temperatures of compounds B-8, B-10, B-12, and B-14 show a notable similarity, indicating a nearly linear relationship between N-I transitions across the B-8 to B-14 homologues.

The consistency of transition temperatures in this series is further corroborated by DSC thermal analysis. Examination of Table 2 indicates that all compounds in the series possess melting points within an intermediate range. As evident from Table 2, the B-n series compounds exhibit an enantiotropic nature. Thus, the series can be predominantly characterized as nematogenic. Figure 6 presents the lengths of mesophases throughout the entire B-n compound series. The range of temperatures for the nematic phase spans from 4.8°C to 30.9°C, with a recorded thermal stability of 145°C. Notably, the nematic mesophase lengths of the B-3 and B-9 homologues show significant resemblance. However, none of the homologues exhibit a smectic phase.

**POM texture characterization:** The synthesized series investigated in this research paper displays a diverse array of mesomorphic properties, meticulously examined through polarizing optical microscopy. A thorough comparison was undertaken, juxtaposing these properties with established mesogenic textures, bolstered by a suite of analytical methods. This comprehensive approach facilitated precise characterization of each homologue within the series.

While the majority of the compounds exhibit a nematic characteristic, exceptions were noted for higher homologues such as B-2, B-8, B-10 and B-14 with transition temperatures of 154.3°C, 123°C, 108.8°C and 102.5 °C respectively. Notably, distinct textures emerged within the nematic mesophase at specific temperatures, prompting a comparison with documented liquid crystal textures and subsequent determination of probable alignments for each observed texture.[13], [14]

**Frontier molecular orbitals and molecular electrostatic potential:** The difference in energy levels between frontier molecular orbitals (FMOs), namely the highest occupied molecular orbital (HOMO) and the lowest unoccupied molecular orbital (LUMO), has a significant impact on optical communications, telecommunications, and signal processing applications. Moreover, accurately estimating the energy difference between FMOs is crucial for predicting various essential parameters such as polarizability ( $\alpha$ ), global softness (S), and chemical hardness ( $\eta$ ). Extensive studies have demonstrated the profound influence of the energy gap within FMOs on these parameters.[15]-[18]. The energy difference between the frontier molecular orbitals (FMOs) in compound B-1 is shown in Figure 8. The table also shows that the length of the terminal alkoxy chain did not significantly affect the FMO energy gap or global softness.

## CONCLUSION

This study explores a newly synthesized series of compounds, designated as B-n, and investigates their liquid crystal properties comprehensively. The research yields several key insights:

The B-n series exhibits nematogenic mesophases. A comparative analysis with the PCOCCA-n series highlights that the structural flexibility and molecular rigidity of the

compounds significantly influence their mesomorphic characteristics. The B-n homologues demonstrate intermediate melting points and relatively extended mesophase durations.

- The B-n series exhibits predominant nematogenic behavior, whereas the PCOCCA-n series demonstrates partial smectogenic and entirely nematogenic characteristics.
- For the B-n series, smectogenic properties not visible, whereas in the PCOCCA-n series, smectogenic behavior is observed starting from the ethyloxy homologue.
- Nematogenic behavior is initiated from the ethyloxy homologue in the B-n and in PCOCCA-n series it starts from methoxy homologue.
- Both the B-n and PCOCCA-n series display fully enantiotropic nature.
- The average transition temperatures for the homologous series B-n and PCOCCA-n are detailed in Table 4.
- Based on Table 5, the following conclusions can be drawn:
- B-n series is mesomorphic while PCOCCA-n series can be identified as poly mesomorphic, displaying both smectic and nematic mesophases.
- The nematic mesophase in the PCOCCA-n and B-n series begins with the C1 and B2 homologue respectively.
- The B-n series demonstrates higher thermal stability than the PCOCCA-n series.
- The overall length of the mesophase in the B-n series is shorter than in the PCOCCA-n series.

## ACKNOWLEDGEMENT

The authors express their gratitude to the Department of Chemistry at Saurashtra University, Rajkot, for their support of this research, which was funded by DST-FIST and sponsored by UGC-SAP. Special thanks are extended to Dr. A.V. Doshi, former Principal of M.V.M. Science and Home Science College, Rajkot, for his invaluable assistance during this investigation. Additionally, we appreciate the National Facility for Drug Discovery through New Chemical Entities (NCEs) for their help in analyzing the samples.

**Conflict of Interest Statement:** The authors declare that there is no conflict of interest regarding the publication of this paper.

**Source of Funding:** This research was supported by Saurashtra University, The funders had no role in the design of the study; in the collection, analysis, and interpretation of data; in the writing of the manuscript; or in the decision to publish the results.

## REFERENCES

- Ravalia, S. U. M. R. Dube, and U. C. Bhoya, "Molecular structural flexibility dependence of mesomorphism through ortho-substituted nitro group," *World Sci News*, vol. 159, pp. 59–70, 2021.
- Lowe, A. M. N. L. Abbott, and S.-T. Ha, "Liquid Crystalline Materials for Biological Applications," *Chem Mater*, vol. 24, no. 5, pp. 746–758, 2012.
- Lockwood N. A. and N. L. Abbott, "Self-Assembly of Surfactants and Phospholipids at Interfaces Between

- Aqueous Phases and Thermotropic Liquid Crystals,” *Curr Opin Colloid Interface Sci*, vol. 10, pp. 111–120, 2005.
- Lagerwall J. P. F. and G. Scalia, “A new era for liquid crystal research: Applications of liquid crystals in soft matter nano-, bioand microtechnology,” *Curr Appl Phys*, vol. 12, no. 6, pp. 1387–1412, 2012.
- Bai Y. and N. L. Abbott, “Recent Advances in Colloidal and Interfacial Phenomena Involving Liquid Crystals,” *Langmuir*, vol. 27, pp. 5719–5738, 2011.
- Al-Rubaie L. A. A. R. and R. J. Mhessn, “Synthesis and characterization of azo dye para red and new derivatives,” *E-J Chem*, vol. 9, no. 1, pp. 465–470, 2012.
- Kiliç M. and Z. Çinar, “Structures and mesomorphic properties of cyano-containing calamitic liquid crystal molecules,” *J Mol Struct Theochem*, vol. 808, pp. 53–61, 2007.
- Gray, G. W. *Thermotropic liquid crystals*, 1st ed. New York (NY): John Wiley and Sons, 1987.
- Ghanem E. and S. Al-Hariri, “Synthesis and powder X-ray diffraction of new Schiff-base liquid crystal,” *Liq Cryst Today*, vol. 22, no. 4, pp. 76–81, 2013.
- Dave, J. S. V. R. A., and R. A., “Mesomorphic Behaviour of the Cholesteryl Esters-I: p-n-Alkoxybenzoates of Cholesterol,” in *Liquid Crystals and Ordered Fluids*, 1970, pp. 477–487. doi: 10.1007/978-1-4684-8214-0\_38.
- Kemme, S. T. T. Šmejkal, and B. Breit, “Practical Synthesis of (E)- $\alpha$ ,  $\beta$ -Unsaturated Carboxylic Acids Using a One-Pot Hydroformylation/Decarboxylative Knoevenagel Reaction Sequence,” *Adv Synth Catal*, vol. 350, no. 7–8, pp. 989–994, 2008, doi: 10.1002/adsc.200700592.
- Neises B. and W. Steglich, “Simple method for the esterification of carboxylic acids,” *Angew Chem Int Ed Engl*, vol. 17, no. 7, pp. 522–524, 1978.
- Sarkar, D. D. “Cholesterol-based dimeric liquid crystals: synthesis, mesomorphic behaviour of frustrated phases and DFT study,” *Liq Cryst*, vol. 40, no. 4, pp. 468–481, 2013.
- Karim, M. R. “Synthesis and characterization of azo benzothiazole chromophore based liquid crystal macromers: effects of substituents on benzothiazole ring and terminal group on mesomorphic, thermal and optical properties,” *Mater Chem Phys*, vol. 140, no. 2–3, pp. 543–552, 2013.
- Saad M. A. H. A. and G. R. Saad, “New calamitic thermotropic liquid crystals of 2-hydroxypyridine ester mesogenic core: mesophase behaviour and DFT calculations,” *Liq Cryst*, vol. 47, no. 1, pp. 114–124, 2019, doi: 10.1080/02678292.2019.1631967.
- Alhaddad M. A. H. A. and O. A. Alhaddad, “Experimental and theoretical approaches of molecular geometry and mesophase behaviour relationship of laterally substituted azopyridines,” *Liq Cryst*, vol. 46, no. 9, pp. 1440–1451, 2019, doi: 10.1080/02678292.2019.1581290.
- Alhaddad, H. A. H. M. Ahmed, and O. A. Alhaddad, “New chair shaped supramolecular complexes-based aryl nicotinate derivative; mesomorphic properties and DFT molecular geometry,” *RSC Adv*, vol. 9, no. 29, pp. 16366–16374, 2019, doi: 10.1039/c9ra02558h.
- Saad H. A. and G. R. Saad, “Synthesis and mesophase behaviour of Schiff base/ester 4-(arylideneamino)phenyl-4'-alkoxy benzoates and their binary mixtures,” *J Mol Liq*, vol. 273, pp. 266–273, 2019, doi: 10.1016/j.molliq.2018.10.035.

\*\*\*\*\*